PHOTONICS Research

N-polar InGaN nanowires: breaking the efficiency bottleneck of nano and micro LEDs

Xianhe Liu,[1,2,†] Yi Sun,[1,†] Yakshita Malhotra,[1] Ayush Pandey,[1] Ping Wang,[1] Yuanpeng Wu,[1] Kai Sun,[3] and Zetian Mi[1,*]

[1]Department of Electrical Engineering and Computer Science, University of Michigan, Ann Arbor, Michigan 48109, USA
[2]Guangzhou Institute of Technology, Xidian University, Guangzhou 510555, China
[3]Department of Materials Science and Engineering, University of Michigan, Ann Arbor, Michigan 48109, USA
*Corresponding author: ztmi@umich.edu

Received 14 September 2021; revised 27 November 2021; accepted 13 December 2021; posted 16 December 2021 (Doc. ID 443165); published 1 February 2022

The efficiency of conventional quantum well light-emitting diodes (LEDs) decreases drastically with reducing areal size. Here we show that such a critical size scaling issue of LEDs can be addressed by utilizing N-polar InGaN nanowires. We studied the epitaxy and performance characteristics of N-polar InGaN nanowire LEDs grown on sapphire substrate by plasma-assisted molecular beam epitaxy. A maximum external quantum efficiency ~11% was measured for LEDs with lateral dimensions as small as 750 nm directly on wafer without any packaging. The effect of electron overflow and Auger recombination on the device performance is also studied. This work provides a viable approach for achieving high-efficiency nano and micro LEDs that were not previously possible.

https://doi.org/10.1364/PRJ.443165

1. INTRODUCTION

The microelectronic industry has benefited tremendously from the miniaturization of transistors, e.g., MOSFETs, down to dimensions below 10–100 nm scale. Shrinking the sizes of optoelectronic devices, e.g., light-emitting diodes (LEDs) and laser diodes to micro- and nanoscale, however, severely deteriorates the device performance. For example, while external quantum efficiency (EQE) in the range of 50%–80% can be commonly measured under current densities of 1–26 A/cm^2 for large-area InGaN blue quantum well LEDs with lateral dimensions on the order of tens to hundreds of micrometers, the efficiency is substantially reduced for nano- and microscale devices [1–19]. Schematically shown in Fig. 1 are some previously reported efficiency values for InGaN LEDs with various sizes and emission colors [1–19]. The difficulty of realizing high-efficiency micro LEDs has been considered one of the major roadblocks for next-generation mobile display, sensing, imaging, and biomedicine applications [20–30]. Moreover, there are virtually no reports on meaningful efficiency values for LEDs with sizes below 1 μm. Fundamental challenges include the surface damage induced by etching in the fabrication process and the resulting severe nonradiative surface recombination and poor charge carrier transport and injection in the device's active region [31–33].

Alternatively, LEDs can be fabricated utilizing nanostructures synthesized by the bottom-up approach. Due to the efficient surface strain relaxation, such nanostructures are largely free of dislocations and exhibit epitaxially smooth surface [34–36]. In this context, significant attention has been paid to InGaN nanowire-based devices in the past decade. Full-color emission has been demonstrated for InGaN nanowires grown in a single epitaxy step by controlling their size and spacing, thereby enabling transfer-free monolithic full-color LED arrays [23,37,38]. Quantum dot-in-nanowires, core-shell heterostructures, and tunnel junctions have also been developed to reduce nonradiative surface recombination and to significantly enhance charge carrier injection efficiency [39–42]. To date, however, these studies have been largely focused on Ga-polar structures, which are often characterized by the presence of pyramid-like surface morphology when grown along the *c* axis [37,43]. Moreover, there have been few reports on the performance and efficiency for such devices at the micro- and nanoscale [44].

Recent advances have shown that N-polar structures can offer significant performance advantages compared to their Ga-polar counterparts. N-polar III-nitrides can be grown at relatively higher temperatures, thereby significantly reducing the formation of point defects, which is critical for achieving high-efficiency emission in the deep visible [45]. N-polar InGaN nanowires grown along the *c* axis exhibit a flat top surface, which can greatly simplify the device fabrication process and improve the yield. Studies have also suggested that N-polar InGaN LEDs can exhibit reduced electron overflow and are

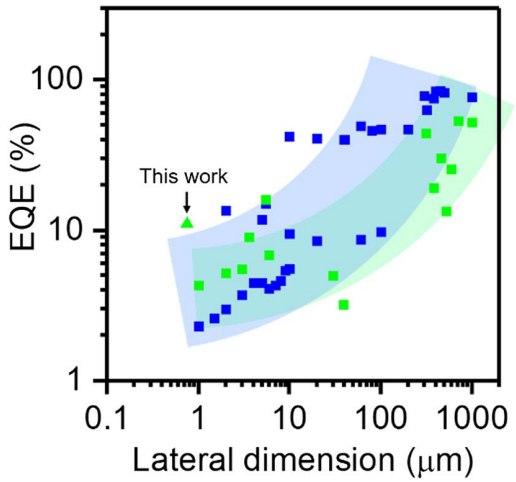

Fig. 1. Variations of peak EQE of InGaN/GaN LEDs versus lateral dimension for some reported devices in the literature, showing the significantly reduced efficiency with decreasing device size [1–19]. The current density corresponding to the peak EQE varies in the range of ~1–26 A/cm^2. Blue square: blue LEDs. Green square: green LEDs.

therefore well suited for high power operation [46]. Moreover, N-polar III-nitride nanostructures can be grown under N-rich epitaxy conditions, which can enable efficient p-type conduction by suppressing N vacancy related defect formation [47,48]. Previous studies of N-polar LEDs, however, were largely focused on spontaneously grown nanowires with random distribution of size, spacing, and morphology. To the best of our knowledge, there has been no report on site-controlled N-polar InGaN nanowire LEDs in the visible [49–51].

In this context, we report on the demonstration of high-efficiency N-polar InGaN nanowire submicrometer LEDs operating at the green wavelength. N-polar InGaN nanowires with the incorporation of multiple InGaN quantum disks were grown on a N-polar GaN template on sapphire substrate. A maximum EQE ~11% was measured for LEDs with dimensions as small as 750 nm directly on wafer without any packaging. Detailed analysis also shows that the room temperature internal quantum efficiency (IQE) is in the range of 60% for a green-emitting nanowire LED at an injection current density ~1 A/cm^2. The effect of electron overflow and Auger recombination on the device performance is also studied. This study provides a viable approach to address the size scaling issue associated with conventional quantum well LEDs, thereby enabling high-efficiency nano and micro LEDs that were not previously possible.

2. GROWTH AND FABRICATION

The N-polar GaN templates were grown on sapphire substrate using a Veeco GENxplor plasma-assisted molecular beam epitaxial (PAMBE) system. Sufficient nitridation of the substrate was first performed *in situ* at 400°C. Then a GaN buffer layer was grown at 650°C. The N-polar GaN epilayer had a thickness ~800 nm and was doped n-type with Si.

To perform selective area epitaxy (SAE) on N-polar GaN templates, a patterning process is adopted, schematically shown in Figs. 2(a) and 2(b) [52–55]. A 10 nm thick Ti layer was first deposited by electron beam evaporation, which was followed by electron beam lithography and dry etching of Ti. The resist was then removed, and the patterns were thoroughly cleaned for growth. The schematic of the patterned substrate with periodic array of openings in the Ti layer is illustrated in Fig. 2(b). The growth was performed in a Veeco Gen 930 PAMBE system. Nitridation of the substrate with patterned Ti mask was first performed *in situ* at 400°C for 10 min to avoid the formation of cracks of the Ti mask during growth. Under optimized conditions, epitaxy of GaN was suppressed on the surface of Ti mask due to the high desorption rate of Ga adatoms, thereby allowing for growth only in the openings as illustrated in Fig. 2(c). The device structure is schematically shown in the inset of Fig. 2(c), which includes an n-GaN nanowire template, an active region consisting of six stacks of InGaN quantum disks and AlGaN barriers, a p-AlGaN layer, and a p-GaN layer. The n-GaN nanowire template was grown using a Ga beam equivalent pressure (BEP) of ~4×10^{-7} Torr and a nitrogen flow rate of 0.7 sccm at a pyrometer temperature of 670°C. The InGaN/AlGaN quantum disk active region was grown at a reduced temperature of 500°C measured by pyrometer. The subsequent growth of p-Ga(Al)N was performed using a Ga BEP of ~4×10^{-7} Torr and an Al BEP of 8.7×10^{-9} Torr, and a nitrogen flow rate of 0.64 sccm at a temperature of 670°C. The p-AlGaN layer is designed to be ~20 nm thick. The incorporation of Al in the barriers and the p-AlGaN layer promotes the formation of an Al-rich

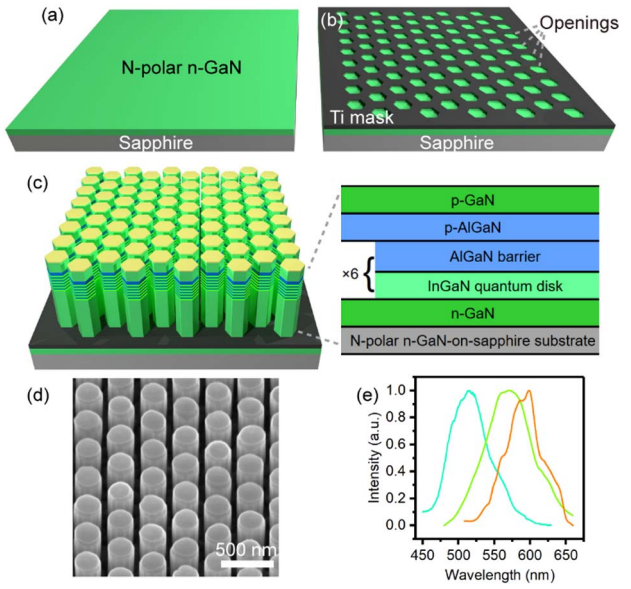

Fig. 2. (a) Schematic of a N-polar GaN template grown on sapphire substrate. (b) Schematic of a patterned N-polar n-GaN template on sapphire using Ti mask. (c) Schematic of InGaN/GaN nanowires formed by selective area epitaxy. Inset: schematic of the LED heterostructure. (d) Scanning electron microscopy (SEM) image of the nanowires. (e) Photoluminescence spectra measured from InGaN nanowires with various indium compositions in the quantum disk active region.

AlGaN shell, which can significantly reduce nonradiative surface recombination and enable high-efficiency emission [56].

The fabrication of micro LEDs started with surface passivation of the nanowires. 50 nm Al_2O_3 was deposited by atomic layer deposition at 250°C and then etched back with inductively coupled plasma to reveal the top part of nanowires for p-metal contact deposition. The Al_2O_3 layer on the nanowire sidewalls remained for passivation purposes. An additional SiO_2 layer was deposited by plasma-enhanced chemical vapor deposition. Submicrometer current injection windows on top of nanowire crystals were made using standard lithography and dry etching of SiO_2 and Al_2O_3. The current injection window for n-metal contact deposition on the template was formed simultaneously. Then a stack of 5 nm Ni/5 nm Au/180 nm indium tin oxide was deposited on the nanowires and annealed at 550°C for 1 min in 5% H_2 and 95% N_2 ambient. A stack of 5 nm Ti/30 nm Au was deposited on the N-polar n-GaN template to serve as the n-contact. To enhance light extraction, top reflecting layers consisting of 50 nm Ag, 150 nm Al, and 50 nm Au were deposited on the device's top surface.

3. RESULTS AND DISCUSSION

A. Material Characterizations

The N-polar nanowires formed in this process exhibit highly uniform dimension and morphology, shown in Fig. 2(d), which is in direct contrast to the uncontrolled properties for previously reported N-polar nanowires by spontaneous growth process [34,57,58]. The nanowires formed by SAE maintain the same polarity as the GaN template. Unlike Ga-polar nanowires, N-polar nanowires have a flat morphology on the top, which is the polar *c* plane. Therefore, the InGaN quantum disks are expected to reside on the polar plane, which is similar to that of conventional InGaN quantum well LED devices, except without the formation of extensive defects and dislocations. The emission wavelengths can be controllably tuned by varying the compositions and/or sizes of the disks as shown by representative spectra in Fig. 2(e) exhibiting different peak positions and colors. The photoluminescence measurements were performed at room temperature using a 405 nm laser with an incident power of ~5 mW. The cyan and green color emissions in Fig. 2(e) were achieved from two nanowire arrays on the same sample grown under the aforementioned condition by exploiting the geometry-dependent In incorporation previously demonstrated by Sekiguchi *et al.* and Ra *et al.* [23,38]. The orange emission in Fig. 2(e) was achieved from another sample using a higher (1.4 sccm) nitrogen flow rate to enhance In incorporation with other conditions remaining identical.

The structural properties were characterized for a calibration nanowire sample exhibiting green emission using scanning transmission electron microscopy (STEM). Shown in Fig. 3(a) is a high angle annular dark field (HAADF) image of one nanowire. The nanowire clearly exhibits a flat morphology due to the N-polarity. The relatively light gray layers are the InGaN quantum disks, and the relatively dark gray layers correspond to the AlGaN barriers. A high-magnification image around the active region is shown in Fig. 3(b).

To reveal the structure of the active region, energy-dispersive X-ray spectroscopy was performed for the distribution

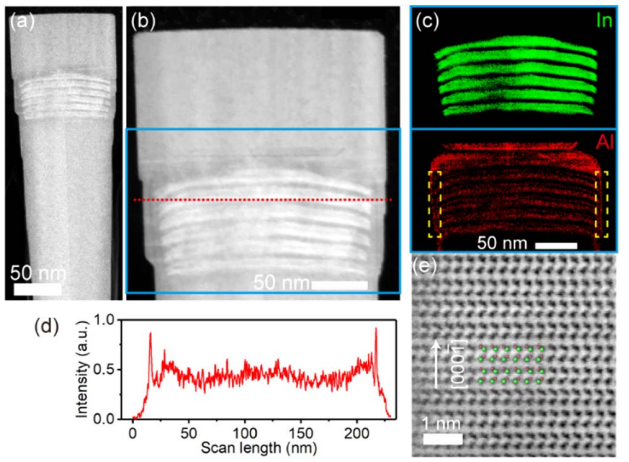

Fig. 3. (a) STEM-HAADF image of a single InGaN/AlGaN nanowire with six stacks of InGaN quantum disks exhibiting green emission. (b) High magnification of the region around the quantum disks. (c) Elemental mapping of In and Al in the region denoted by the blue box in (b). (d) The profile of Al distribution along the red dashed line in (b). (e) High-magnification STEM annular bright-field image showing the atomic stack order, where green circles represent Ga and red circles represent N.

of In and Al in the region in the blue box in Fig. 3(b). The top panel in Fig. 3(c) confirms the formation of vertically stacked InGaN quantum disks. Unlike conventional InGaN quantum wells, which commonly have disorders, such InGaN quantum disks in nanowires exhibited extensive atomic ordering [59]. Comparing with the distribution of Al in the bottom panel of Fig. 3(c), there is clearly spatial overlap between the distributions of In and Al. The thickness of each In-containing layer is designed to be ~6–7 nm, but the actual thickness may vary, depending on the lateral indium migration as well as interfacial atom diffusion. It is also seen that the In distribution of the bottom three InGaN layers exhibits a relatively dark region, suggesting a low In content in these regions, which may further contribute to the linewidth broadening of the emission spectra. Furthermore, the distribution of Al in the bottom panel of Fig. 3(c) clearly exhibits Al-rich shell structure indicated by the yellow dashed boxes. This Al-rich AlGaN shell is also visible in Fig. 3(b), which has vertical dark gray lines surrounding the InGaN quantum disks near the sidewall of the nanowire. Such an Al-rich AlGaN shell structure can effectively confine charge carriers in the InGaN quantum disks and substantially minimize surface nonradiative recombination on the sidewalls, leading to enhanced emission efficiency [56]. A line scan for the Al distribution was performed along the red dashed line in Fig. 3(b). The signal intensity in Fig. 3(d) exhibits two pronounced peaks near the surface of the nanowire, which further confirms the presence of an Al-rich AlGaN shell. The spontaneous formation of such an Al-rich AlGaN shell is driven by the different surface migration lengths of Al adatoms. As Al adatoms have shorter migration lengths than Ga and In adatoms, those impinging on the sidewalls cannot reach the top flat surface but rather bond with N locally. However, most Ga and In adatoms can efficiently migrate to the top flat surface and contribute to epitaxy in

the vertical direction, leading to Ga/In deficiency on the sidewalls. The resultant Al-rich shell is critical for suppressing surface nonradiative recombination and enhancing light output [42,56]. It is important to note that Ga-polar nanowires with typical pyramid top morphology also exhibit an Al-rich shell structure, which is however formed differently along the semi-polar planes [60]. Individual Ga and N atoms, denoted by green and red circles, respectively, are clearly resolved in a high-resolution image, shown in Fig. 3(e), which further confirms the N-polarity of InGaN nanostructures in this study.

B. Current-Voltage Characteristics and Emission Efficiency

The current-voltage (*I-V*) characteristics are shown in Fig. 4(a). A turn-on voltage of ~4.5 V was measured with a negligibly small reverse bias leakage, suggesting the well-formed junction. The relatively high turn-on voltage is partly related to the etching of the top p-GaN layer during the fabrication process and the resulting large contact resistance. The turn-on voltage can be reduced by optimizing the fabrication process. A relatively high current density of ~350 A/cm^2 can be readily reached at 7 V, indicating efficient charge-carrier transport in the N-polar nanowires. The calculated current density considers the real size of the current injection window as shown in the inset of Fig. 4(a) and the fill factor of the nanowire array. It is seen that only approximately four nanowires were located within this current injection window. Given that no degradation of *I-V* characteristics was seen for such small devices at a relatively high bias, our nanowires prove to be suited for relatively high-power and high-brightness operation. The leakage current under reverse bias is very low, which is close to the measurement limit of our instrument. Electroluminescence spectra with a main peak at ~530 nm were measured at room temperature as shown in Fig. 4(b). A weak shoulder at 563 nm, which is likely due to the size dispersion of the disks, is also measured at a low current density. As the current density increases, the main peak becomes dominant and remains stable with a small peak wavelength shift from 530 to 524 nm and a slight broadening of full width at half-maximum from 36.6 to 37.8 nm. Both the peak shift and spectral broadening with injection current are substantially improved compared to conventional Ga-polar quantum well LEDs [7,61]. The inset of Fig. 4(b) shows the device under room light illumination. Further optimization in the InGaN growth condition is expected to improve the homogeneity among InGaN disks and thereby eliminate any parasitic emission.

The output power and EQE were measured by directly placing the device on a Si detector. A Keithley 2400 was used as the sourcemeter for current injection. A Si detector (Newport 818-ST2-UV/DB) together with a power meter (Newport 1919-R) was used for the output power measurement. During the measurements, the device was placed on top of the Si detector, and light emitted from the backside of the sapphire substrate was collected and recorded. Shown in Fig. 5(a), the output power showed a nearly linear increase with injection current. Variations of the EQE with current are shown in Fig. 5(b). The measured EQE showed a rapid increase with injection current and reached a peak value of ~11% at a relatively small current density of 0.83 A/cm^2, indicating a small contribution from Shockley–Read–Hall recombination or surface nonradiative recombination. This variation of EQE is similar to conventional high-efficiency quantum well LEDs. The reduced quantum confinement Stark effect (QCSE) associated with N-polarity nanowires may not be the dominant factor for the high EQE because our Ga-polar nanowire device exhibits a lower EQE of ~5.5% despite that the active region resides on the semi-polar planes with less QCSE [62]. The EQE, however, exhibited a drop by half when the current density reached 12.6 A/cm^2. The severe efficiency droop can be partly explained by the presence of significant electron overflow as described below.

C. Analysis on the Light Emission Efficiency

The ABC model with an additional term DN^4 was used to analyze the LED performance. Considering the small dimensions of the device and the resultant heating effect under high bias, only data below 30 A/cm^2 were used for analysis. By assuming 1×10^{-11} cm^3 s^{-1} for B and an equivalent total disk thickness of 40 nm [63,64], other coefficients can be estimated as follows: $A = 1.37 \times 10^6$ s^{-1}, $C = 6.97 \times 10^{-32}$ cm^6 s^{-1}, and $D = 2.27 \times 10^{-47}$ cm^9 s^{-1}. The variation of the contribution from each term is shown in Fig. 6. A relatively high peak IQE of ~60% is derived, which is comparable to some of the relatively high IQE values reported in the literature for InGaN epilayers and nanowires [65–71]. It is seen that the contributions from CN^3 and DN^4 become quickly dominant as the current reaches ~6–7 A/cm^2, confirming the presence of significant electron overflow, which was indicated by the fast drop of measured EQE. Therefore, the device efficiency can be

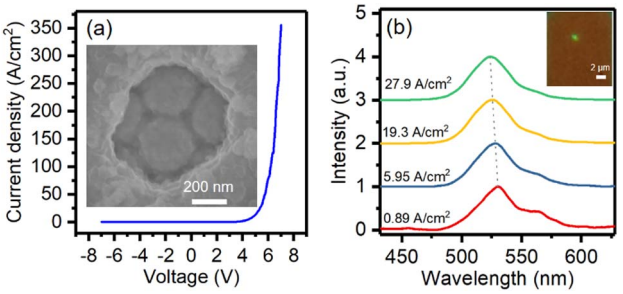

Fig. 4. (a) *I-V* characteristics of a submicrometer InGaN nanowire LED. Inset: SEM image of the current injection window of the device. (b) Representative electroluminescence spectra of a N-polar submicrometer LED. Inset: optical microscopy image of the device.

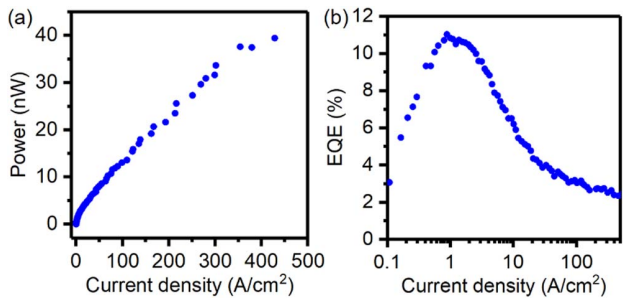

Fig. 5. Variations of (a) output power and (b) EQE with current density.

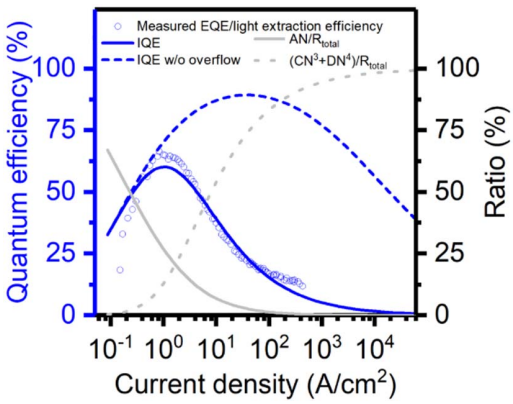

Fig. 6. Left axis: IQE (solid blue curve) derived based on the ABC model analysis. The estimated IQE (blue circles) based on the measured EQE divided by the light extraction efficiency is also shown for comparison. Right axis: estimated contribution of AN (light gray solid curve) and $CN^3 + DN^4$ (light gray dotted curve) to the total recombination rate. The IQE, or maximum achievable EQE (dashed blue curve) is further estimated for a well-designed InGaN nanowire LED assuming negligible electron overflow, showing a peak IQE ~89%.

further enhanced, and the peak EQE can occur at higher current density upon the improvement of device structure and reduction of electron overflow by optimizing the doping level and the electron blocking layer or superlattice structure. As shown in the inset of Fig. 4(a), such nanoscale LEDs consist of only few nanowires, with approximately half of them being partially contacted. The highly asymmetric injection of electrons and holes is expected to lead to a more severe electron overflow effect than a conventional device. Such a critical issue can be addressed through proper patterning and design, which will lead to further enhanced EQE. It is worthwhile to mention that the heating effect in the local region on the submicrometer scale also contributes to the efficiency droop, which can be minimized by reducing the device resistance with further optimization of fabrication process and device structure.

Based on these studies, we have further analyzed the performance limit for such N-polar InGaN nanowire micro LEDs. For a well-designed device, it is expected that the efficiency droop will be predominantly determined by Auger recombination. For an Auger coefficient ~2.6×10^{-31} $cm^6 s^{-1}$, as commonly reported for InGaN quantum wells [72], the maximum IQE is estimated to be ~89% at room temperature, shown as the dashed blue curve in Fig. 6. The maximum achievable EQE is estimated to be >60%, assuming a modestly high light extraction efficiency ~70% with proper device packaging. It is also noticed that the peak IQE occurs at an injection current density ~38 A/cm^2, which is significantly higher than that of conventional InGaN quantum well LEDs. This is due to the use of relatively thicker InGaN quantum wells/disks in the active region. The thicker disks can reduce carrier density (N) for the same injection current, thereby leading to reduced efficiency droop caused by Auger recombination ($\propto N^3$). This is one of the principal advantages of InGaN nanowires, as relatively thick quantum wells/disks can be incorporated in InGaN nanowires without generating extensive defects and dislocations. Such thick active region is favorable for high output power operation under high current injection. Together with the minimization of defect density and surface nonradiative recombination by N-polar nanowire structure and Al-rich shell, high efficiency can be expected under both low current injection and high current injection.

4. CONCLUSION

In conclusion, we have demonstrated that N-polar InGaN nanowires can enable high-efficiency submicrometer-scale LEDs that were not previously possible. The peak IQE is estimated to be ~60% by fitting with ABC model. Our detailed analysis further suggests that N-polar nano and micro LEDs can exhibit maximum achievable EQE potentially exceeding 60% in the deep visible upon full optimization of material quality, carrier injection, and light extraction in the future, which is nearly one order of magnitude higher than that by conventional quantum well devices. The device performance can be further improved by optimizing the design and fabrication process and by utilizing the special technique of tunnel junction. With high efficiency and ultrastable operation, N-polar nanowires have emerged as suitable building blocks for future ultrahigh-resolution, ultrahigh-efficiency mobile displays, TVs, and virtual reality systems.

Funding. University of Michigan; NS Nanotech Inc.

Acknowledgment. The authors are thankful for the discussions with Dr. David Laleyan, Mr. Matthew Stevenson, and Dr. Seth Coe-Sullivan from NS Nanotech, Inc.

Disclosures. Zetian Mi: NS Nanotech, Inc. (F, I, P, S). The University of Michigan and Mi have a financial interest in NS Nanotech, Inc.

Data Availability. The data that support the findings of this study are available from the corresponding author upon reasonable request.

†These authors contributed equally to this work.

REFERENCES

1. A. I. Alhassan, R. M. Farrell, B. Saifaddin, A. Mughal, F. Wu, S. P. DenBaars, S. Nakamura, and J. S. Speck, "High luminous efficacy green light-emitting diodes with AlGaN cap layer," Opt. Express **24**, 17868–17873 (2016).
2. J. Bai, Y. Cai, P. Feng, P. Fletcher, C. Zhu, Y. Tian, and T. Wang, "Ultrasmall, ultracompact and ultrahigh efficient InGaN micro light emitting diodes (μLEDs) with narrow spectral line width," ACS Nano **14**, 6906–6911 (2020).
3. J.-X. Guo, J. Ding, C.-L. Mo, C.-D. Zheng, S. Pan, and F.-Y. Jiang, "Effect of AlGaN interlayer on luminous efficiency and reliability of GaN-based green LEDs on silicon substrate," Chin. Phys. B **29**, 047303 (2020).
4. R. Hashimoto, J. Hwang, S. Saito, and S. Nunoue, "High-efficiency green-yellow light-emitting diodes grown on sapphire (0001) substrates," Phys. Status Solidi C **10**, 1529–1532 (2013).
5. D. Hwang, A. Mughal, C. D. Pynn, S. Nakamura, and S. P. DenBaars, "Sustained high external quantum efficiency in ultrasmall blue III–nitride micro-LEDs," Appl. Phys. Express **10**, 032101 (2017).

6. S. Kimura, H. Yoshida, K. Uesugi, T. Ito, A. Okada, and S. Nunoue, "Performance enhancement of blue light-emitting diodes with InGaN/GaN multi-quantum wells grown on Si substrates by inserting thin AlGaN interlayers," J. Appl. Phys. **120**, 113104 (2016).
7. P. P. Li, Y. B. Zhao, H. J. Li, J. M. Che, Z. H. Zhang, Z. C. Li, Y. Y. Zhang, L. C. Wang, M. Liang, X. Y. Yi, and G. H. Wang, "Very high external quantum efficiency and wall-plug efficiency 527 nm InGaN green LEDs by MOCVD," Opt. Express **26**, 33108–33115 (2018).
8. C. D. Pynn, S. J. Kowsz, S. H. Oh, H. Gardner, R. M. Farrell, S. Nakamura, J. S. Speck, and S. P. DenBaars, "Green semipolar III-nitride light-emitting diodes grown by limited area epitaxy," Appl. Phys. Lett. **109**, 041107 (2016).
9. H. Sato, R. B. Chung, H. Hirasawa, N. Fellows, H. Masui, F. Wu, M. Saito, K. Fujito, J. S. Speck, S. P. DenBaars, and S. Nakamura, "Optical properties of yellow light-emitting diodes grown on semipolar $(11\bar{2}2)$ bulk GaN substrates," Appl. Phys. Lett. **92**, 221110 (2008).
10. J. M. Smith, R. Ley, M. S. Wong, Y. H. Baek, J. H. Kang, C. H. Kim, M. J. Gordon, S. Nakamura, J. S. Speck, and S. P. DenBaars, "Comparison of size-dependent characteristics of blue and green InGaN microLEDs down to 1 μm in diameter," Appl. Phys. Lett. **116**, 071102 (2020).
11. J. J. Wierer, A. David, and M. M. Megens, "III-nitride photonic-crystal light-emitting diodes with high extraction efficiency," Nat. Photonics **3**, 163–169 (2009).
12. S. Yamamoto, Y. Zhao, C.-C. Pan, R. B. Chung, K. Fujito, J. Sonoda, S. P. DenBaars, and S. Nakamura, "High-efficiency single-quantum-well green and yellow-green light-emitting diodes on semipolar $(20\bar{2}1)$ GaN substrates," Appl. Phys. Express **3**, 122102 (2010).
13. B. P. Yonkee, E. C. Young, S. P. DenBaars, S. Nakamura, and J. S. Speck, "Silver free III-nitride flip chip light-emitting-diode with wall plug efficiency over 70% utilizing a GaN tunnel junction," Appl. Phys. Lett. **109**, 191104 (2016).
14. T. Shioda, H. Yoshida, K. Tachibana, N. Sugiyama, and S. Nunoue, "Enhanced light output power of green LEDs employing AlGaN interlayer in InGaN/GaN MQW structure on sapphire (0001) substrate," Phys. Status Solidi A **209**, 473–476 (2012).
15. C. A. Hurni, A. David, M. J. Cich, R. I. Aldaz, B. Ellis, K. Huang, A. Tyagi, R. A. DeLille, M. D. Craven, F. M. Steranka, and M. R. Krames, "Bulk GaN flip-chip violet light-emitting diodes with optimized efficiency for high-power operation," Appl. Phys. Lett. **106**, 031101 (2015).
16. Y. Narukawa, M. Ichikawa, D. Sanga, M. Sano, and T. Mukai, "White light emitting diodes with super-high luminous efficacy," J. Phys. D **43**, 354002 (2010).
17. Y. Narukawa, J. Narita, T. Sakamoto, K. Deguchi, T. Yamada, and T. Mukai, "Ultra-high efficiency white light emitting diodes," Jpn. J. Appl. Phys. **45**, L1084–L1086 (2006).
18. Y. Narukawa, M. Sano, M. Ichikawa, S. Minato, T. Sakamoto, T. Yamada, and T. Mukai, "Improvement of luminous efficiency in white light emitting diodes by reducing a forward-bias voltage," Jpn. J. Appl. Phys. **46**, L963–L965 (2007).
19. R. T. Ley, J. M. Smith, M. S. Wong, T. Margalith, S. Nakamura, S. P. DenBaars, and M. J. Gordon, "Revealing the importance of light extraction efficiency in InGaN/GaN microLEDs via chemical treatment and dielectric passivation," Appl. Phys. Lett. **116**, 251104 (2020).
20. H. X. Jiang and J. Y. Lin, "Nitride micro-LEDs and beyond - a decade progress review," Opt. Express **21**, A475–A484 (2013).
21. T. Wu, C.-W. Sher, Y. Lin, C.-F. Lee, S. Liang, Y. Lu, S.-W. Huang Chen, W. Guo, H.-C. Kuo, and Z. Chen, "Mini-LED and micro-LED: promising candidates for the next generation display technology," Appl. Sci. **8**, 1557 (2018).
22. H. Xu, J. Zhang, K. M. Davitt, Y. K. Song, and A. V. Nurmikko, "Application of blue–green and ultraviolet micro-LEDs to biological imaging and detection," J. Phys. D **41**, 094013 (2008).
23. Y.-H. Ra, R. Wang, S. Y. Woo, M. Djavid, S. M. Sadaf, J. Lee, G. A. Botton, and Z. Mi, "Full-color single nanowire pixels for projection displays," Nano Lett. **16**, 4608–4615 (2016).
24. Z. Liu, W. C. Chong, K. M. Wong, and K. M. Lau, "GaN-based LED micro-displays for wearable applications," Microelectron Eng. **148**, 98–103 (2015).
25. D. Peng, K. Zhang, V. S.-D. Chao, W. Mo, K. M. Lau, and Z. Liu, "Full-color pixelated-addressable light emitting diode on transparent substrate (LEDoTS) micro-displays by CoB," J. Display Technol. **12**, 742–746 (2016).
26. X. Zhang, P. Li, X. Zou, J. Jiang, S. H. Yuen, C. W. Tang, and K. M. Lau, "Active matrix monolithic LED micro-display using GaN-on-Si epilayers," IEEE Photon. Technol. Lett. **31**, 865–868 (2019).
27. N. McAlinden, Y. Cheng, R. Scharf, E. Xie, E. Gu, C. Reiche, R. Sharma, P. Tathireddy, P. Tathireddy, L. Rieth, S. Blair, and K. Mathieson, "Multisite microLED optrode array for neural interfacing," Neurophotonics **6**, 035010 (2019).
28. D. Tsonev, H. Chun, S. Rajbhandari, J. J. D. McKendry, S. Videv, E. Gu, M. Haji, S. Watson, A. E. Kelly, G. Faulkner, M. D. Dawson, H. Haas, and D. O. Brien, "A 3-Gb/s single-LED OFDM-based wireless VLC link using a gallium nitride μLED," IEEE Photon. Technol. Lett. **26**, 637–640 (2014).
29. M. S. Wong, S. Nakamura, and S. P. DenBaars, "Review—progress in high performance III-nitride micro-light-emitting diodes," ECS J. Solid State Sci. Technol. **9** (2020).
30. H. Li, M. S. Wong, M. Khoury, B. Bonef, H. Zhang, Y. Chow, P. Li, J. Kearns, A. A. Taylor, P. De Mierry, Z. Hassan, S. Nakamura, and S. P. DenBaars, "Study of efficient semipolar (11-22) InGaN green micro-light-emitting diodes on high-quality (11-22) GaN/sapphire template," Opt. Express **27**, 24154–24160 (2019).
31. F. Olivier, S. Tirano, L. Dupré, B. Aventurier, C. Largeron, and F. Templier, "Influence of size-reduction on the performances of GaN-based micro-LEDs for display application," J. Lumin. **191**, 112–116 (2017).
32. M. Minami, S. Tomiya, K. Ishikawa, R. Matsumoto, S. Chen, M. Fukasawa, F. Uesawa, M. Sekine, M. Hori, and T. Tatsumi, "Analysis of GaN damage induced by Cl_2/$SiCl_4$/Ar plasma," Jpn. J. Appl. Phys. **50**, 08JE03 (2011).
33. R. J. Shul, L. Zhang, A. G. Baca, C. G. Willison, J. Han, S. J. Pearton, and F. Ren, "Inductively coupled plasma-induced etch damage of GaN p-n junctions," J. Vac. Sci. Technol. A **18**, 1139–1143 (2000).
34. H. P. T. Nguyen, M. Djavid, K. Cui, and Z. Mi, "Temperature-dependent nonradiative recombination processes in GaN-based nanowire white-light-emitting diodes on silicon," Nanotechnology **23**, 194012 (2012).
35. K. Kishino and S. Ishizawa, "Selective-area growth of GaN nanocolumns on Si(111) substrates for application to nanocolumn emitters with systematic analysis of dislocation filtering effect of nanocolumns," Nanotechnology **26**, 225602 (2015).
36. M. Mandl, X. Wang, T. Schimpke, C. Kölper, M. Binder, J. Ledig, A. Waag, X. Kong, A. Trampert, F. Bertram, J. Christen, F. Barbagini, E. Calleja, and M. Strassburg, "Group III nitride core–shell nano- and microrods for optoelectronic applications," Phys. Status Solidi RRL **7**, 800–814 (2013).
37. K. Kishino, N. Sakakibara, K. Narita, and T. Oto, "Two-dimensional multicolor (RGBY) integrated nanocolumn micro-LEDs as a fundamental technology of micro-LED display," Appl. Phys. Express **13**, 014003 (2019).
38. H. Sekiguchi, K. Kishino, and A. Kikuchi, "Emission color control from blue to red with nanocolumn diameter of InGaN/GaN nanocolumn arrays grown on same substrate," Appl. Phys. Lett. **96**, 231104 (2010).
39. H. P. T. Nguyen, S. Zhang, A. T. Connie, M. G. Kibria, Q. Wang, I. Shih, and Z. Mi, "Breaking the carrier injection bottleneck of phosphor-free nanowire white light-emitting diodes," Nano Lett. **13**, 5437–5442 (2013).
40. M. Pristovsek, Y. Han, T. Zhu, M. Frentrup, M. J. Kappers, C. J. Humphreys, G. Kozlowski, P. Maaskant, and B. Corbett, "Low defect large area semi-polar $(11\bar{2}2)$ GaN grown on patterned (113) silicon," Phys. Status Solidi B **252**, 1104–1108 (2015).
41. T. Wang, "Topical review: development of overgrown semi-polar GaN for high efficiency green/yellow emission," Semicond. Sci. Technol. **31**, 093003 (2016).
42. S. M. Sadaf, Y. H. Ra, H. P. T. Nguyen, M. Djavid, and Z. Mi, "Alternating-current InGaN/GaN tunnel junction nanowire white-light emitting diodes," Nano Lett. **15**, 6696–6701 (2015).
43. X. Liu, Y. Wu, Y. Malhotra, Y. Sun, and Z. Mi, "Micrometer scale InGaN green light emitting diodes with ultra-stable operation," Appl. Phys. Lett. **117**, 011104 (2020).

44. K. Kishino and K. Yamano, "Green-light nanocolumn light emitting diodes with triangular-lattice uniform arrays of InGaN-based nanocolumns," IEEE J. Quantum Electron. **50**, 538–547 (2014).
45. A. Uedono, K. Shojiki, K. Uesugi, S. F. Chichibu, S. Ishibashi, M. Dickmann, W. Egger, C. Hugenschmidt, and H. Miyake, "Annealing behaviors of vacancy-type defects in AlN deposited by radio-frequency sputtering and metalorganic vapor phase epitaxy studied using monoenergetic positron beams," J. Appl. Phys. **128**, 085704 (2020).
46. F. Akyol, D. N. Nath, S. Krishnamoorthy, P. S. Park, and S. Rajan, "Suppression of electron overflow and efficiency droop in N-polar GaN green light emitting diodes," Appl. Phys. Lett. **100**, 111118 (2012).
47. N. H. Tran, B. H. Le, S. Zhao, and Z. Mi, "On the mechanism of highly efficient p-type conduction of Mg-doped ultra-wide-bandgap AlN nanostructures," Appl. Phys. Lett. **110**, 032102 (2017).
48. Y. Wu, D. A. Laleyan, Z. Deng, C. Ahn, A. F. Aiello, A. Pandey, X. Liu, P. Wang, K. Sun, E. Ahmadi, Y. Sun, M. Kira, P. K. Bhattacharya, E. Kioupakis, and Z. Mi, "Controlling defect formation of nanoscale AlN: toward efficient current conduction of ultrawide-bandgap semiconductors," Adv. Electron. Mater. **6**, 2000337 (2020).
49. M. Brubaker, K. Genter, J. Weber, B. Spann, A. Roshko, P. Blanchard, T. Harvey, and K. Bertness, "Core-shell p-i-n GaN nanowire LEDs by N-polar selective area growth," Proc. SPIE **10725**, 1072502 (2018).
50. M. D. Brubaker, K. L. Genter, A. Roshko, P. T. Blanchard, B. T. Spann, T. E. Harvey, and K. A. Bertness, "UV LEDs based on p–i–n core–shell AlGaN/GaN nanowire heterostructures grown by N-polar selective area epitaxy," Nanotechnology **30**, 234001 (2019).
51. M. D. Brubaker, S. M. Duff, T. E. Harvey, P. T. Blanchard, A. Roshko, A. W. Sanders, N. A. Sanford, and K. A. Bertness, "Polarity-controlled GaN/AlN nucleation layers for selective-area growth of GaN nanowire arrays on Si(111) substrates by molecular beam epitaxy," Cryst. Growth Des. **16**, 596–604 (2016).
52. Ž. Gačević, D. G. Sánchez, and E. Calleja, "Formation mechanisms of GaN nanowires grown by selective area growth homoepitaxy," Nano Lett. **15**, 1117–1121 (2015).
53. K. Kishino, H. Sekiguchi, and A. Kikuchi, "Improved Ti-mask selective-area growth (SAG) by rf-plasma-assisted molecular beam epitaxy demonstrating extremely uniform GaN nanocolumn arrays," J. Cryst. Growth **311**, 2063–2068 (2009).
54. X. Liu, B. H. Le, S. Y. Woo, S. Zhao, A. Pofelski, G. A. Botton, and Z. Mi, "Selective area epitaxy of AlGaN nanowire arrays across nearly the entire compositional range for deep ultraviolet photonics," Opt. Express **25**, 30494–30502 (2017).
55. H. Sekiguchi, K. Kishino, and A. Kikuchi, "Ti-mask selective-area growth of GaN by RF-plasma-assisted molecular-beam epitaxy for fabricating regularly arranged InGaN/GaN Nanocolumns," Appl. Phys. Express **1**, 124002 (2008).
56. H. P. T. Nguyen, M. Djavid, S. Y. Woo, X. Liu, A. T. Connie, S. Sadaf, Q. Wang, G. A. Botton, I. Shih, and Z. Mi, "Engineering the carrier dynamics of InGaN nanowire white light-emitting diodes by distributed p-AlGaN electron blocking layers," Sci. Rep. **5**, 7744 (2015).
57. K. Hestroffer, C. Leclere, C. Bougerol, H. Renevier, and B. Daudin, "Polarity of GaN nanowires grown by plasma-assisted molecular beam epitaxy on Si(111)," Phys. Rev. B **84**, 245302 (2011).
58. H. P. T. Nguyen, K. Cui, S. Zhang, S. Fathololoumi, and Z. Mi, "Full-color InGaN/GaN dot-in-a-wire light emitting diodes on silicon," Nanotechnology **22**, 445202 (2011).
59. S. Y. Woo, M. Bugnet, H. P. T. Nguyen, Z. Mi, and G. A. Botton, "Atomic ordering in InGaN alloys within nanowire heterostructures," Nano Lett. **15**, 6413–6418 (2015).
60. X. Liu, Y. Sun, Y. Malhotra, A. Pandey, Y. Wu, K. Sun, and Z. Mi, "High efficiency InGaN nanowire tunnel junction green micro-LEDs," Appl. Phys. Lett. **119**, 141110 (2021).
61. C. Du, Z. Ma, J. Zhou, T. Lu, Y. Jiang, P. Zuo, H. Jia, and H. Chen, "Enhancing the quantum efficiency of InGaN yellow-green light-emitting diodes by growth interruption," Appl. Phys. Lett. **105**, 071108 (2014).
62. S. Zhao, S. Y. Woo, M. Bugnet, X. Liu, J. Kang, G. A. Botton, and Z. Mi, "Three-dimensional quantum confinement of charge carriers in self-organized AlGaN nanowires: a viable route to electrically injected deep ultraviolet lasers," Nano Lett. **15**, 7801–7807 (2015).
63. S. A. A. Muyeed, W. Sun, M. R. Peart, R. M. Lentz, X. Wei, D. Borovac, R. Song, N. Tansu, and J. J. Wierer, Jr., "Recombination rates in green-yellow InGaN-based multiple quantum wells with AlGaN interlayers," J. Appl. Phys. **126**, 213106 (2019).
64. T. H. Ngo, B. Gil, B. Damilano, K. Lekhal, and P. De Mierry, "Internal quantum efficiency and Auger recombination in green, yellow and red InGaN-based light emitters grown along the polar direction," Superlattices Microstruct. **103**, 245–251 (2017).
65. C. Zhao, T. K. Ng, C.-C. Tseng, J. Li, Y. Shi, N. Wei, D. Zhang, G. B. Consiglio, A. Prabaswara, A. A. Alhamoud, A. M. Albadri, A. Y. Alyamani, X. X. Zhang, L.-J. Li, and B. S. Ooi, "InGaN/GaN nanowires epitaxy on large-area MoS_2 for high-performance light-emitters," RSC Adv. **7**, 26665–26672 (2017).
66. S. Deshpande and P. Bhattacharya, "An electrically driven quantum dot-in-nanowire visible single photon source operating up to 150 K," Appl. Phys. Lett. **103**, 241117 (2013).
67. S. Jahangir, A. Banerjee, and P. Bhattacharya, "Carrier lifetimes in green emitting InGaN/GaN disks-in-nanowire and characteristics of green light emitting diodes," Phys. Status Solidi C **10**, 812–815 (2013).
68. W. Guo, M. Zhang, A. Banerjee, and P. Bhattacharya, "Catalyst-free InGaN/GaN nanowire light emitting diodes grown on (001) silicon by molecular beam epitaxy," Nano Lett. **10**, 3355–3359 (2010).
69. A. G. Sarwar, S. D. Carnevale, F. Yang, T. F. Kent, J. J. Jamison, D. W. McComb, and R. C. Myers, "Semiconductor nanowire light-emitting diodes grown on metal: a direction toward large-scale fabrication of nanowire devices," Small **11**, 5402–5408 (2015).
70. H. P. T. Nguyen, S. Zhang, K. Cui, X. Han, S. Fathololoumi, M. Couillard, G. A. Botton, and Z. Mi, "p-type modulation doped InGaN/GaN dot-in-a-wire white-light-emitting diodes monolithically grown on Si(111)," Nano Lett. **11**, 1919–1924 (2011).
71. M. M. Muhammed, N. Alwadai, S. Lopatin, A. Kuramata, and I. S. Roqan, "High-efficiency InGaN/GaN quantum well-based vertical light-emitting diodes fabricated on β-Ga_2O_3 substrate," ACS Appl. Mater. Interfaces **9**, 34057–34063 (2017).
72. F. Olivier, A. Daami, C. Licitra, and F. Templier, "Shockley-Read-Hall and Auger non-radiative recombination in GaN based LEDs: a size effect study," Appl. Phys. Lett. **111**, 022104 (2017).